



ELSEVIER

Available online at www.sciencedirect.com

SCIENCE @ DIRECT®

Nonlinear Analysis 63 (2005) e155–e164

**Nonlinear
Analysis**

www.elsevier.com/locate/na

Evolution of chaotic regions in control parameter planes depending on hysteretic dissipation

J. Awrejcewicz^{a,*}, L.P. Dzyubak^b

^a*Department of Automatics and Biomechanics, Technical University of Lodz, 1/15 Stefanowskiego St., 90-924 Lodz, Poland*

^b*Department of Applied Mathematics, Kharkov Polytechnic University, 21 Frunze St., 61002 Kharkov, Ukraine*

Abstract

Using an effective algorithm based on analysis of the wandering trajectories, chaotic behavior regions of oscillators with hysteresis are obtained in various parametric planes. Substantial influence of a hysteretic dissipation value on the form and location of these regions and also restraining and generating effects of the hysteretic dissipation on a chaos occurrence are demonstrated.

© 2005 Elsevier Ltd. All rights reserved.

Keywords: Hysteresis; Chaos; Masing and Bouc–Wen oscillators

1. Introduction

Hysteresis is a well-known phenomenon in many fields of science and is caused by very different processes. The models describing systems with hysteresis are discontinuous and contain high nonlinearities with memory-dependent properties. Investigation of these systems within the framework of approximate analytical approaches as, for instant, slowly varying parameters or harmonic balance methods, results in the conclusion that independently of values of control parameters residing in conditions of an external periodic excitation the hysteretic system has a stable symmetric asymptotic response. However, the

* Corresponding author. Tel./fax: +48 42 6312225.

E-mail address: awrejcew@p.lodz.pl (J. Awrejcewicz).

¹ This work has been supported by the J. Mianowski Foundation of Polish Science Support, as well as the Polish Scientific Research Committee (KBN) under Grant no 5 T07A 019 23 and the Central European University in Budapest.

recent publications and works [5,6], based on both numerical and combined numerical-analytical techniques, present frequency–response curves and bifurcation diagrams which point to the presence of solutions and bifurcations mostly unexpected for hysteretic oscillators. However, the control parameter spaces of such systems are not sufficiently studied. In this connection, the prediction of the behavior of the systems with hysteresis depending on various parameters is very topical.

Often during a simulation of hysteresis, a system is considered as a black box and an *output* (or a response) of the system is modelled using analytical expressions or differential equations supposing that the *input* of the system is known [7,9]. Though various transient processes of the *input* may be reflected in a minor loops formation, as a rule, regular signals of *inputs* are considered and regular responses of the system are expected. However, as investigations show, a hysteretic dissipation can change conditions for the possibility of chaotic response occurrence substantially.

In the present work, the classical Masing and Bouc-Wen hysteretic oscillators are considered. Among standard procedures of diagnosing or prediction of chaotic behavior of a system under investigation the computation of the spectrum of Lyapunov exponents is a straightforward but computationally intensive method [8] (especially in the case of many-parametric non-smooth systems such as oscillators with hysteresis). It not infrequently results in some problems in practice. On the one hand, the individual terms of the cumulative product matrix grow exponentially, and, on the other hand, the eigenvectors all tend to align in the direction of maximum growth and hence do not accurately span the space. To avoid these problems, the Gram–Schmidt reorthonormalization may be used additionally increasing the time consumed and complicating the algorithm. In this work, to predict conditions for regular/unregular behavior of the hysteretic oscillators under harmonic excitation, an effective algorithm devoted to numerical analysis of these systems is applied. This technique is based on analysis of the wandering trajectories and already had been successfully applied to the cases of smooth and non-smooth systems in Refs. [1–4,8]. The applied approach is simpler and faster from a computational point of view compared with standard procedures (some advantages are reported, for example, in [2]) and permits sufficient accuracy in tracing regular/unregular responses of the hysteretic systems. Since the domains of chaotic behavior of hysteretic systems have a complex structure with periodic “windows” and with a set of scattered points, the analytical estimation cannot guarantee precise threshold estimation.

The motion of each oscillator is described by the coupled differential sets and all components of motion have influence on each other. Restraining and generating effects of the hysteretic dissipation on a chaotic behavior occurring in various parametric planes are demonstrated.

2. Chaotic and regular behavior of the Masing and Bouc-Wen oscillators

Let us consider classical hysteretic models such as Masing oscillator and Bouc-Wen oscillator. In both cases, an external periodic excitation with an amplitude F and frequency Ω acts on the mass m which oscillates along an inertial base. These oscillators possess hysteretic properties and it is supposed that there is a linear viscous damper with a coefficient 2μ .

The following set of differential equations governs a motion of the Masing oscillator:

$$\begin{aligned} \dot{x} &= y, \\ \dot{y} &= -2\mu y - (1 - \nu)g(x) - \nu z + F \cos \Omega t, \\ \dot{z} &= g' \left(\frac{z - z_i}{2} \right) y. \end{aligned} \tag{1}$$

In the above,

$$\nu \in [0, 1]; \quad g(x) = \frac{(1 - \delta)x}{(1 + |x|^n)^{1/n}} + \delta x; \quad R = (1 - \nu)g(x) + \nu z$$

is total restoring force with non-linear elastic part $(1 - \nu)g(x)$ and with hysteretic part νz . The case $\nu = 1$ corresponds to maximum hysteretic dissipation and $\nu = 0$ corresponds to elastic behavior of the oscillator. The parameter δ characterizes a ratio between the post- and pre-yielding stiffness. The parameter n governs the smoothness of the transitions from the elastic to the plastic range. Couples $\pm(x_i, z_i)$ represent the velocity reversal points at $\dot{x} = 0$. According to Masing’s rule which is disseminated on the case of steady-state motion of the hysteretic oscillator, the loading/unloading branches of a hysteresis loop are similar geometrically. So, if $f(x, z) = 0$ is the equation of a virgin loading curve, then the equations $f((x \pm x_i)/2, (z \pm z_i)/2) = 0$ describe loading/unloading branches of the hysteresis loop. In the case of non-steady-state motion of the Masing’s oscillator, it is supposed that the equation of any hysteretic response curve can be obtained by applying the original Masing rule to the virgin loading curve using the latest point of velocity reversal.

A motion of Bouc-Wen oscillator is governed by the following set of differential equations:

$$\begin{aligned} \dot{x} &= y, \\ \dot{y} &= -2\mu y - \delta x - (1 - \delta)z + F \cos \Omega t, \\ \dot{z} &= [k_z - (\gamma + \beta \operatorname{sgn}(y)\operatorname{sgn}(z))|z|^n]y, \end{aligned} \tag{2}$$

where $R = \delta x + (1 - \delta)z$ is the total restoring force; the parameters $(k_z, \beta, n) \in R^+$ and $\gamma \in R$ govern the shape of the hysteresis loop. The parameters δ and n have the same sense as in the case of the Masing model.

Let us describe briefly the approach based on analysis of the wandering trajectories in view of the state vector of the systems (1), (2) for $\mathbf{x} \in R^3$. A chaotic behavior of nonlinear deterministic systems supposes a wandering of trajectories of motion around the various equilibrium states. They are characterized by unpredictability and sensitive dependence on the initial conditions. By analyzing trajectories of motion of these systems, it is possible to find the chaotic vibration regions in control parameters space.

The continuous dependence property on the initial conditions $\mathbf{x}^{(0)} = \mathbf{x}(t_0)$ of a solution of the set (1) or (2) will be used: for every initial condition $\mathbf{x}^{(0)}, \tilde{\mathbf{x}}^{(0)} \in R^3$, for every number $T > 0$, no matter how large, and for every preassigned arbitrary small $\varepsilon > 0$, it is

possible to indicate a positive number $\delta > 0$, such that if the distance ρ between $\mathbf{x}^{(0)}$ and $\tilde{\mathbf{x}}^{(0)}$, $\rho(\mathbf{x}^{(0)}, \tilde{\mathbf{x}}^{(0)}) < \delta$, and $|t| \leq T$, the following inequality is satisfied:

$$\rho(\mathbf{x}(t), \tilde{\mathbf{x}}(t)) < \varepsilon.$$

That is, if the initial points are chosen close enough, then during the preassigned arbitrary large time interval $-T \leq t \leq T$, the distance between simultaneous positions of moving points will be less given positive number ε .

For the sake of tracing chaotic and regular dynamics, it is supposed that with the increase in time all trajectories remain in the closed bounded domain of a phase space, i.e.

$$\exists C_i \in R: \max_t |x_i(t)| \leq C_i, \quad i = 1, 2, 3.$$

To analyze trajectories of the sets (1) and (2), the characteristic vibration amplitudes A_i of components of the motion are introduced, $A_i = \frac{1}{2} |\max_{t_1 \leq t \leq T} x_i(t) - \min_{t_1 \leq t \leq T} x_i(t)|$. Here and below, index number i runs over three values corresponding to three generalized coordinates x, y , and z . $[t_1, T] \subset [t_0, T]$ and $[t_0, T]$ is the time interval, in which the trajectory is considered. The interval $[t_0, t_1]$ is the time interval, in which all transient processes are damped.

For the sake of our investigation it seems most convenient to use the embedding theorem and to consider a 3-dimensional parallelepiped instead of a hyper-sphere with the center at point \mathbf{x} . Two neighboring initial points $\mathbf{x}^{(0)} = \mathbf{x}(t_0)$ and $\tilde{\mathbf{x}}^{(0)} = \tilde{\mathbf{x}}(t_0)$ ($\mathbf{x} = (x, y, z)^T$ or $\mathbf{x} = (x_1, x_2, x_3)^T$) are chosen in the 3-dimensional parallelepiped $P_{\delta_x, \delta_y, \delta_z}(\mathbf{x}^{(0)})$ such that $|x_i^{(0)} - \tilde{x}_i^{(0)}| < \delta_i$, where $\delta_i > 0$ is small in comparison with A_i . In the case of regular motion, it is expected that $\varepsilon_i > 0$ used in inequality $|x_i(t) - \tilde{x}_i(t)| < \varepsilon_i$ is also small in comparison with A_i . The wandering orbits attempt to fill up some bounded domain of the phase space. At instant t_0 the neighboring trajectories diverge exponentially afterwards. Hence, for some instant t_1 , the absolute values of differences $|x_i(t) - \tilde{x}_i(t)|$ can take any values in closed interval $[0, 2A_i]$. An auxiliary parameter α is introduced, $0 < \alpha < 1$. αA_i is referred to as divergence measures of observable trajectories in the directions of generalized coordinates and with the aid of parameter α one has been chosen, which is *inadmissible* for the case of “regularity” of the motion. The domains, where a chaotic behavior of considered systems is possible, can be found using the following condition:

$$\exists t^* \in [t_1, T] : |x(t^*) - \tilde{x}(t^*)| > \alpha A_x.$$

If this inequality is satisfied in some nodal point of the sampled control parameter space, then such motion is relative to the chaotic one (including transient and alternating chaos). The manifold of all such nodal points of the investigated control parameter space setup domains of chaotic behavior of the considered systems.

3. Results and discussion

Stability of motion depends on all parameters of the considered hysteretic models including initial conditions. We succeeded sufficiently accurately in tracing unregular

responses of the Masing and Bouc-Wen hysteretic oscillators in the damping coefficient-amplitude and frequency-amplitude of external periodic excitation planes after a coordinate sampling.

The Masing oscillator (1) is non-linear both in the case of a pure elastic behavior without hysteretic dissipation ($\nu = 0$) and in the case of motion with hysteretic dissipation ($\nu > 0$). And at $\nu = 0$, chaos has been found too. Fig. 1 displays the evolution of chaotic behavior domains with increase in hysteretic dissipation value in the mentioned planes. The (Ω, F) and (μ, F) planes had been uniformly sampled by 100×100 nodal points in the rectangles $(0.01 \leq \Omega \leq 0.61; 0.01 \leq F \leq 1.51)$ and $(0.01 \leq \mu \leq 0.26; 0.01 \leq F \leq 1.61)$, respectively. The time period for simulation T is of $300\pi/\Omega$ non-dimensional time units. During computations, one half of the time period T corresponds to the time interval $[t_0, t_1]$, where transient processes are damped. The integration step size is $\pi/100\Omega$. Initial conditions of the closed trajectories are distinguished by 0.5 percent with ratio to characteristic vibration amplitudes, e.g. the starting points of these trajectories are in the 3-dimensional parallelepiped ($|x(t_0) - \tilde{x}(t_0)| < 0.005A_x, |\dot{x}(t_0) - \tilde{\dot{x}}(t_0)| < 0.005A_{\dot{x}}, |z(t_0) - \tilde{z}(t_0)| < 0.005A_z$). The parameter α is chosen to be equal to $\frac{1}{3}$. All domains are multiply connected. There is also some number of scattered points here. Such a structure is characteristic for domains, where chaotic vibrations are possible.

One can observe the effect of restraining the chaotic regions with the increase in the hysteretic dissipation value in the (Ω, F) plane (Fig. 1(a)–(c)). The “quickness” of the restraining decreases when ν increases. So, in the case of maximum hysteretic dissipation value $\nu = 1$, the chaotic regions in the (Ω, F) plane are distinguished from regions (c), Fig. 1, non-principally.

In the (μ, F) plane (Fig. 1(d)–(f)) the form and location of the chaotic domains are changed depending on the hysteretic dissipation that is made conditional upon mutual influence of the nonlinear terms in the set (1).

Fig. 2 characterizes the obtained domains and demonstrates various characteristics of motion of the Masing oscillator as chaos and hysteresis loss (a), and periodic response (b).

Another situation occurs for the Bouc-Wen oscillator (2) which naturally is linear (when $\delta = 1$). So, the hysteretic dissipation adding leads to chaotic responses occurring in this system. Fig. 3 presents the evolution of chaotic behavior regions with the increase in the hysteretic dissipation value in the (Ω, F) and (μ, F) planes. One can observe the changes of the form and location of the chaotic regions. Note that chaotic responses of the Bouc-Wen oscillator are not observed right up to $\delta = 0.2$, when the influence of the nonlinear terms becomes critical. It demonstrates the generating effect of the hysteretic dissipation on chaos occurring in the hysteretic system which appears after some critical value δ_{cr} . After δ_{cr} , both the form and location of the chaotic behavior regions are changed with the increase in the hysteretic dissipation. In the case of maximum hysteretic dissipation value (when $\delta = 0$), the chaotic behavior region in the (Ω, F) plane is almost the same as in case (c), Fig. 3. A “friable” form of the chaotic regions in the (μ, F) planes (d) and (f) is conditioned by the fixation of the frequency $\Omega = 0.24$. Location of the corresponding domains in the (Ω, F) planes are changed with increase in the hysteretic dissipation. The fixed value of Ω only slightly contacts chaotic behavior regions (a) and (c), Fig. 3.

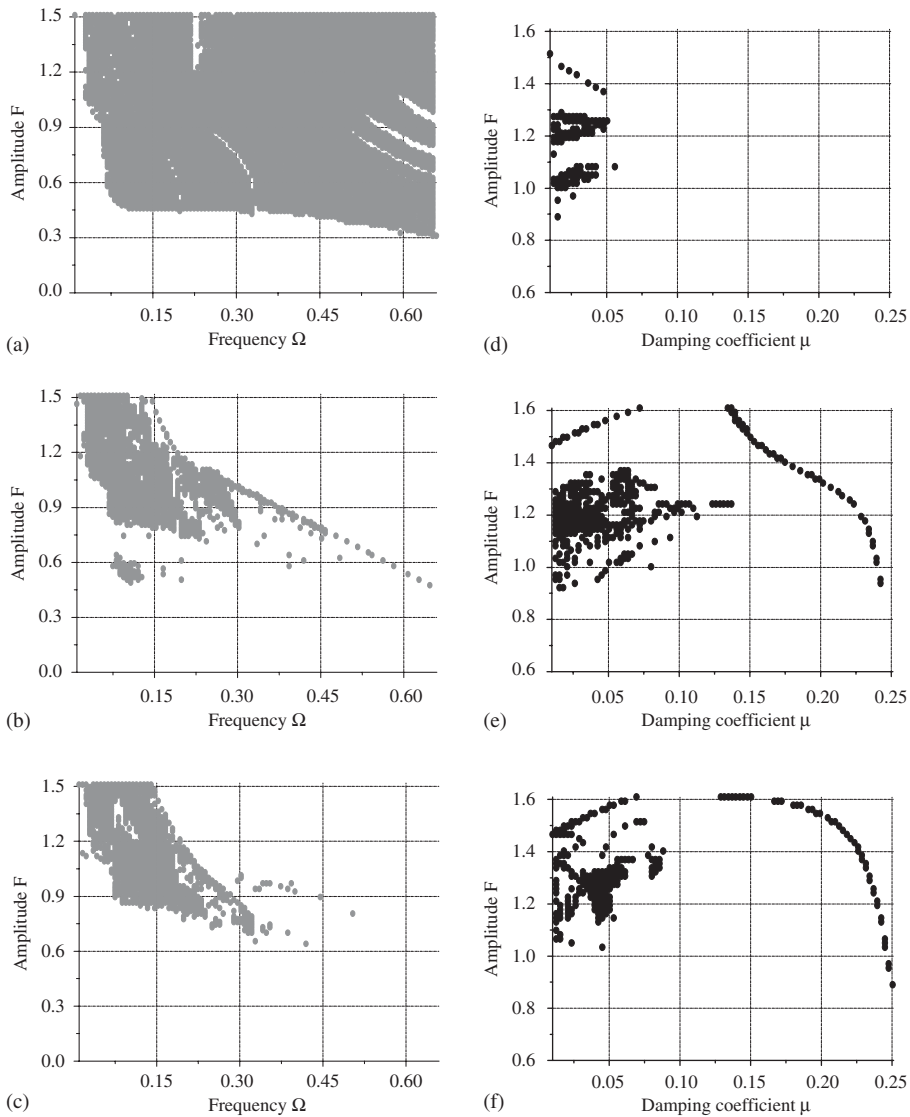


Fig. 1. Evolution of the chaotic regions for the Masing hysteresis model in the (Ω, F) and in the (μ, F) planes with increase in the hysteretic dissipation value (a), (d) $v = 0$; (b), (e) $v = 0.5$; (c), (f) $v = 0.8$. The parameters $\delta = 0.05$, $n = 10.0$, $x(0) = 0.1$, $\dot{x}(0) = 0.1$, $z(0) = 0$ are fixed for all cases, and $\mu = 0$ for cases (a)–(c). $\Omega = 0.15$ for cases (d)–(f).

During simulation, the (Ω, F) and (μ, F) planes had been uniformly sampled by 100×100 nodal points in the rectangles $(0.01 \leq \Omega \leq 0.36; 0.01 \leq F \leq 2.05)$ and $(0.001 \leq \mu \leq 0.04; 0.01 \leq F \leq 1.71)$, respectively. The time period for the simulation T is $300\pi/\Omega$. During

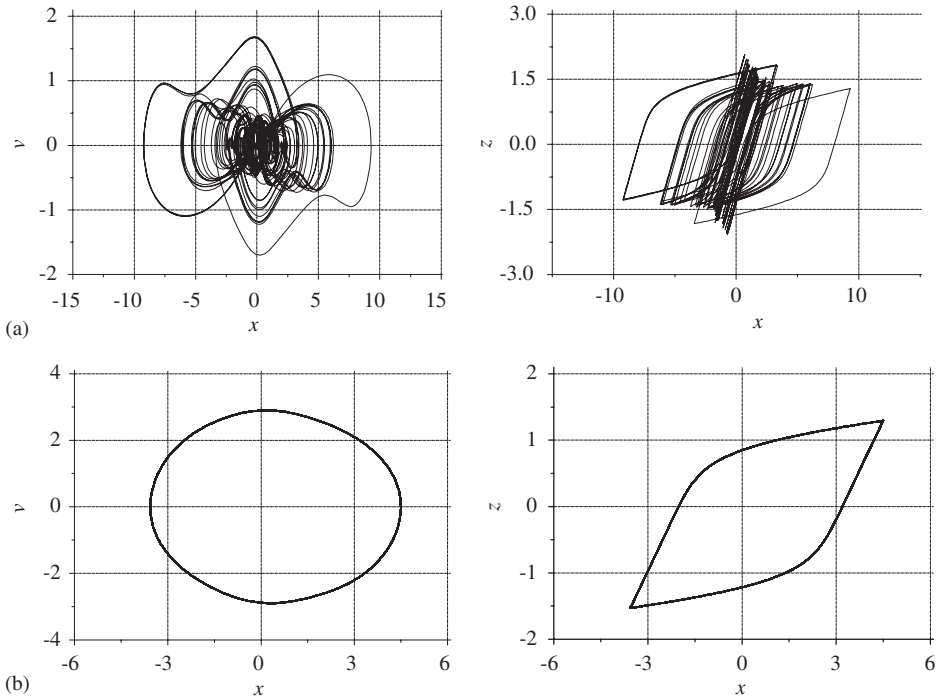


Fig. 2. Phase portraits and hysteresis loops of the Masing hysteretic oscillator in the cases of (a) chaotic ($\Omega=0.15$, $F=1.21$, $\mu=0.026$, $\nu=0.5$, $\delta=0.05$, $n=10.0$, $x(0)=0.1$, $\dot{x}(0)=0.1$, $z(0)=0$) and (b) periodic responses ($\Omega=0.7$, $F=0.8$, $\mu=0$, $\nu=0.5$, $\delta=0.05$, $n=10.0$, $x(0)=0.1$, $\dot{x}(0)=0.1$, $z(0)=0$).

computations, a half of time period corresponds to the time interval $[t_0, t_1]$, where transitional processes are damped. The integration step size is chosen equal to $\pi/40\Omega$. As in the case of the Masing oscillator, the initial conditions of the closed trajectories are distinguished by 0.5 percent with ratio to characteristic vibration amplitudes. The parameter α is set equal to $\frac{1}{3}$.

Fig. 4 characterizes the obtained regions of unregular motion and depicts various responses of the Bouc-Wen oscillator as chaos and hysteresis loss (a), and periodic responses (b) and (c). One can observe in Fig. 4(c), the motion of oscillator with a triple period, and that the hysteresis possesses reduced dissipation properties.

4. Conclusions

Highly nonlinear Masing and Bouc-Wen hysteretic models with discontinuous right-hand sides are investigated using an effective approach based on the analysis of the wandering trajectories [1–4]. This algorithm of quantifying regular and chaotic dynamics is simpler and faster from a computational point of view compared with standard procedures and

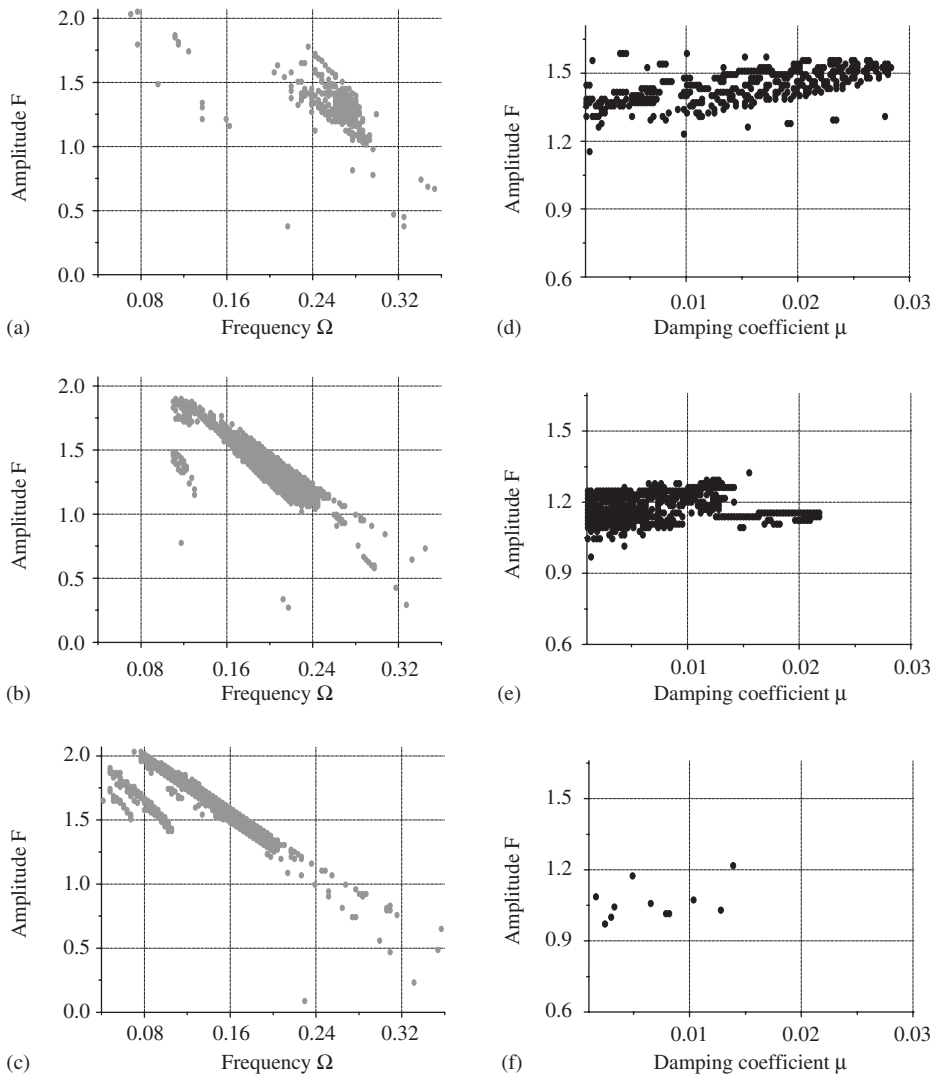


Fig. 3. Evolution of the chaotic regions for the Bouc-Wen oscillator with hysteresis in the (Ω, F) and in the (μ, F) planes with increase in the hysteretic dissipation value (a), (d) $\delta = 0.0476$; (b), (e) $\delta = 0.01$; (c), (f) $\delta = 0.001$ at $k_z = 0.5, \gamma = 0.3, \beta = 0.005, n = 1.0, x(0) = 0.1, \dot{x}(0) = 0.1, z(0) = 0$ and $\mu = 0$ for the cases (a)–(c), $\Omega = 0.24$ for the cases (d)–(f).

allows sufficient in accurately tracing regular/unregular responses of the hysteretic systems. Domains, where chaotic/regular behavior of the oscillators with hysteresis is possible, are found in the damping coefficient-amplitude and the frequency-amplitude of external periodic excitation planes. Substantial influence of a hysteretic dissipation value on the

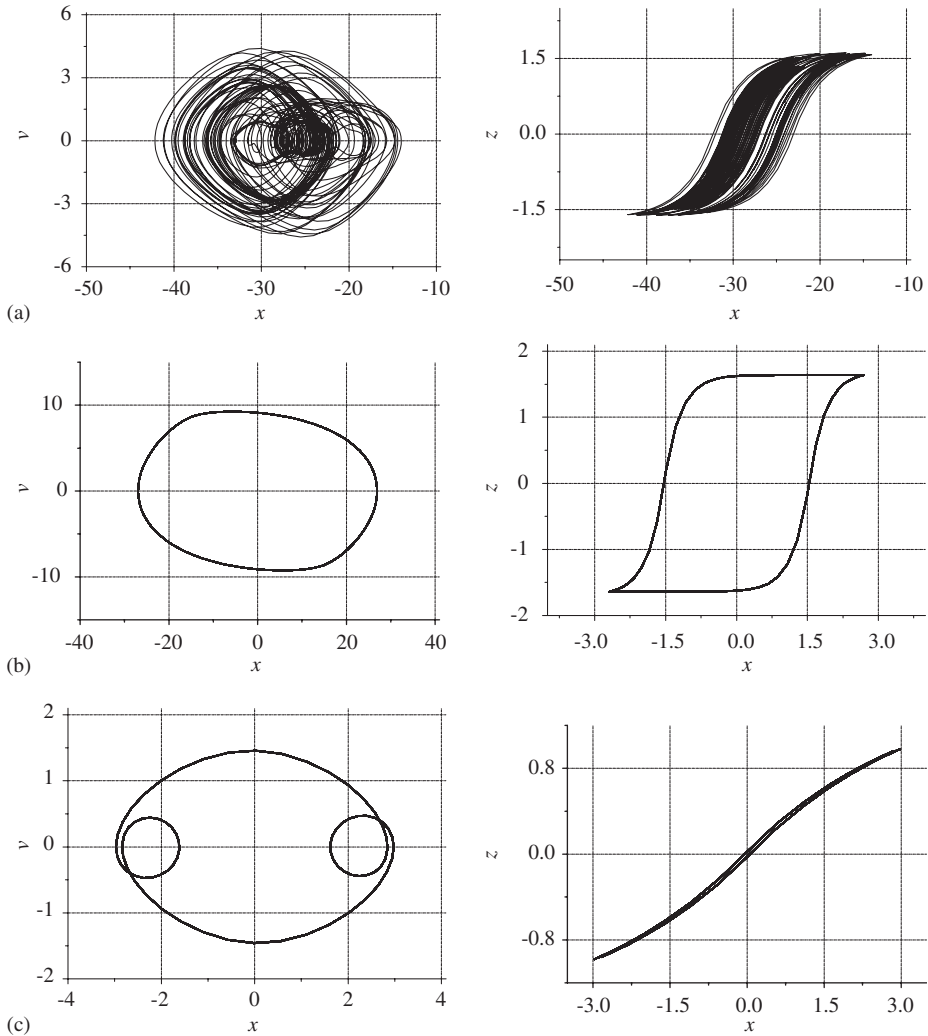


Fig. 4. Phase portraits and hysteresis loops of the Bouc-Wen hysteretic oscillator in the cases of (a) chaotic ($\Omega = 0.24$; $F = 1.1227$, $\mu = 0.00136$, $\delta = 0.01$, $k_z = 0.5$, $\gamma = 0.3$, $\beta = 0.005$, $n = 1.0$, $x(0) = 0.1$, $\dot{x}(0) = 0.1$, $z(0) = 0$) and (b) ($\Omega = 0.35$; $F = 1.2$, $\mu = 0.0$), (c) ($\Omega = 0.2$; $F = 1$, $\mu = 0.0$) periodic responses ($\delta = 0.0476$, $k_z = 0.5$, $\gamma = 0.3$, $\beta = 0.005$, $n = 1.0$, $x(0) = 0.1$, $\dot{x}(0) = 0.1$, $z(0) = 0$).

possibility of chaotic behavior occurring in the systems with hysteresis is shown. Restraining and generating effects of the hysteretic dissipation on a chaotic behavior occurring are demonstrated.

The possibility of the generating effects of hysteretic dissipation on chaos occurring in hysteretic systems which are modelled by means of additional state variables (internal variables) is a subject of further investigations.

References

- [1] J. Awrejcewicz, L. Dzyubak, *Int. J. Nonlinear Sci. Numer. Simul.* 4 (2) (2003) 155.
- [2] J. Awrejcewicz, L. Dzyubak, *Int. J. Bifurcation Chaos*, submitted of publication.
- [3] J. Awrejcewicz, L. Dzyubak, C. Grebogi, *Chaos, Soliton. Fract.* 19 (2004) 503.
- [4] J. Awrejcewicz, R. Mosdorf, *Numerical Analysis of Some Problems of Chaotic Dynamics*, WNT, Warsaw, 2003 (in Polish).
- [5] D. Capecchi, R. Masiani, *Chaos, Soliton. Fract.* 7 (1996) 1583.
- [6] W. Lacarbonara, F. Vestroni, *Nonlinear Dynam.* (2004).
- [7] I.D. Mayergoyz, *Mathematical Models of Hysteresis*, Springer, Berlin, 1991.
- [8] J.C. Sprott, *Chaos and Time-Series Analysis*, Oxford, New York, 2003.
- [9] A. Visintin, *Differential Models of Hysteresis*, Springer, Berlin, 1994.